ethylbenzene, 1,2,4-trimethylbenzene, 1-ethyl-3-vinylbenzene, phenanthrene, 3-methylanisole, methyl benzoate, ethyl benzoate, ethyl 4-ethoxybenzoate, trioxane, 2,5-dimethyl-2,4-hexadiene, 1,5-cyclooctadiene, and the three isomers of xylene, for H_2TPP clathrates of *p*-xylene and *m*-xylene, and for the tetraanisylporphinatozinc(II) clathrate containing *m*-xylene and water (287 pages). Ordering information is given on any current masthead page.

Reaction of Carbon Monoxide with Alkyliron Porphyrins Generated from Alkyl Halides and Electrochemically Produced Iron(I) and Iron("0") Porphyrins

Claire Gueutin,[1a] Doris Lexa,[1a] Michel Momenteau,[1b] and Jean-Michel Savéant*,[1a]

Contribution from the Laboratoire d'Electrochimie Moléculaire de l'Université Paris 7, Unité de Recherche Associée au CNRS No. 438, 2, Place Jussieu, 75251 Paris Cedex 05, France, and Institut Curie, Section de Biologie, Unité INSERM 219, 91405 Orsay, France.
Received June 5, 1989

Abstract: Carbon monoxide inserts in iron–carbon bonds of σ-alkyl porphyrins generated from the reaction of alkyl halides with electrochemically produced low-valent iron porphyrins, with the exception of benzyl derivatives. In the case of σ-aryl complexes, the iron–carbon appears too strong to allow CO insertion. In the case of methyl and other primary alkyls, CO insertion occurs at the Fe(III)–C rather than at the Fe(II)–C oxidation state. Insertion is then accompanied by partial homolysis of the σ-alkyl–Fe(III) complex favored by the binding of CO to the resulting iron(II) porphyrin. The latter reaction prevents the insertion of CO in the iron(III)–*tert*-butyl complex. However, CO then inserts in the Fe(II)–C-*tert*-butyl bond. The reaction mechanism is established and the characteristic rate constants are estimated on the basis of cyclic voltammetry, thin-layer spectroelectrochemistry, and preparative-scale electrolysis.

The reaction of alkyl halides with iron(I)[2a] and iron("0")[2b] porphyrins is a facile route to the corresponding σ-alkyl porphyrin complexes, even with sterically encumbered[2d] carbon and/or iron centers.[2] On the other hand, electrochemical reduction is a convenient way to in situ generate these low-valent complexes from the corresponding iron(III) porphyrins.[2] In a preliminary report,[3a] we have provided evidence that carbon monoxide inserts in the carbon–iron bond of such σ-alkyl porphyrins as in the case of ethyl and *n*-hexyl and of octaethylporphyrin (OEP). It was also shown that insertion occurs with the σ-alkyl complex in its iron(III) oxidation state rather than in its iron(II) oxidation state.[3a] Direct insertion of carbon monoxide in the carbon–iron bond of σ-ethyl-, *n*-butyl-, and neopentyliron(III)–tetraphenylporphyrin complexes obtained from the corresponding alkyllithiums and chloroiron(III) porphyrins has also been demonstrated in an independent preliminary report.[3b]

The purpose of the present paper is to provide a fuller account of the reaction of carbon monoxide with electrochemically generated σ-alkyliron porphyrins as a function of the nature of the alkyl group, so as to precisely determine the conditions under which this "nonmigratory" insertion[3c] can take place and investigate the reaction mechanism. The case of σ-aryliron porphyrins will be also briefly examined.

Results and Discussion

Most of the experiments were carried out with OEP, although a few test experiments were carried out with other porphyrins.

It has been shown, in a previous preliminary report,[3a] that electrolysis of $(OEP)Fe^{III}$ at a potential where the $Fe(I)^-$ complex is generated, in the presence of *n*-hexyl bromide and carbon monoxide, results in the formation of the corresponding iron(II)–acyl complex. The latter was identified by means of its spectral (UV–vis, IR, ^{13}C NMR) and electrochemical (cyclic voltammetry) behavior. Since then, we have found that the same reaction occurs with other primary alkyl halides (the particular case of methyl chloride is discussed below). The acyl complexes thus obtained have the same characteristics as those formed by the reaction of $Fe("0")^{2-}$ porphyrins with carboxylic anhydrides.[5] In this preliminary study,[3a] CO insertion in the primary carbon–iron bond was investigated by cyclic voltammetry and thin-layer spectroelectrochemistry of solutions containing a mixture of the iron(III) porphyrin, the alkyl halide, and carbon monoxide. On the other hand, Goff et al.[3b] investigated the reaction starting from σ-alkyliron(III) porphyrins. In order to investigate the reaction mechanism and kinetics in more detail, we started in the present study from pure solutions of the σ-alkyliron(II) complex. Thanks to the volatility of ethyl bromide, this is most convenient

(1) (a) Université Paris 7. (b) Institut Curie.

(2) (a) Lexa, D.; Mispelter, J.; Savéant, J.-M.; *J. Am. Chem. Soc.* **1981**, *103*, 6806. (b) Lexa, D.; Savéant, J.-M.; Wang, D. L. *Organometallics* **1986**, *5*, 1428. (c) The reaction of alkyl halides with iron(I) porphyrins[2a] yields the $Fe^{III}R$ complex in a first stage. However, this is easier to reduce than the iron(II) porphyrin. Thus, at the potential where the $Fe^{III}R$ complex is produced, it is reduced to the $Fe^{II}R^-$ complex unless other reactions compete favorably. The reductant is in most practical cases the iron(I) complex rather than the electrode since alkylation is not sufficiently fast for the second event to occur. On the other hand, reaction of iron("0") porphyrin with alkyl halides directly yields the $Fe^{II}R^-$ complex. (d) Gueutin, C.; Lexa, D.; Savéant, J.-M.; Wang, D. L. *Organometallics* **1989**, *8*, 1607. (e) For a discussion of the reaction mechanism, dissociative electron transfer followed by bond formation or S_N2 substitution. See ref 2f. (f) Lexa, D.; Savéant, J.-M.; Su, K. B.; Wang, D. L. *J. Am. Chem. Soc.* **1988**, *110*, 7617.

(3) (a) Gueutin, C.; Lexa, D.; Savéant, J.-M.; Momenteau, M. *J. Electroanal. Chem. Interfacial Electrochem.* **1988**, *256*, 219. (b) Arafa, I. M.; Shin, K.; Goff, H. M. *J. Am. Chem. Soc.* **1988**, *110*, 5228. (c) "Nonmigratory"[3b] as opposed to the more common case where the inserting group is coordinated to the metal in cis vis-ā-vis the alkyl group thus allowing an easy intramolecular migration of the latter toward the former.[4]

(4) (a) Alexander, J. J. In *Chemistry of the metal-carbon bond*; Hartley, F. R., Patai, S., Eds.; Interscience: New York, 1985; Vol. 2, p 339. (b) Stoppioni, P.; Dapporte, P.; Sacconi, L. *Inorg. Chem.* **1978**, *17*, 718. (c) Garrou, P. E.; Heck, R. F. *J. Am. Chem. Soc.* **1976**, *98*, 4115.

(5) Gueutin, C.; Lexa, D.; Savéant, J.-M. *J. Electroanal. Chem. Interfacial Electrochem.* **1988**, *256*, 223.

0002-7863/90/1512-1874$02.50/0

carried out in the case of the σ-ethyl complex.

In the absence of EtBr and CO, (OEP)$Fe^{III}Cl$ gives rise, in *N,N'*-dimethylformamide (DMF), to three chemically reversible cyclic voltammetric waves (Figure 1a), corresponding, from positive to negative potentials, to the following three redox couples: Fe(III)/Fe(II) (1/1'), Fe(II)/Fe(I) (2/2'), Fe(I)/Fe("0") (3/3'). Let us first note that, upon addition of CO (1 atm), waves 2/2' both shift cathodically, waves 3/3' remain unaffected, and wave 1' shifts anodically, whereas wave 1 remains at the same place (Figure 1b). This indicates that CO strongly binds to Fe(II) and to neither Fe(III) nor Fe(I).[6]

As shown previously,[2] the σ-alkyl complex can be obtained in its iron(II) oxidation state by reaction of either iron(I) or iron("0") complex with the alkyl halide. In the present case, the σ-alkyliron(II)–OEP complex was prepared by electrolysis of (OEP)-$Fe^{III}Cl$ (1 mM) at −1.6 V vs SCE (corresponding to the generation of iron(I) in the presence of EtBr (2 mM)). Excess EtBr was removed after electrolysis by bubbling argon through the solution. The cyclic voltammogram of the resulting solution is shown in Figure 1c. It consists of an anodic wave (4') and two cathodic waves (5/5' and 6) corresponding to the following reactions:[7a]

$$4' \quad Fe^{III}R - e^- \rightleftharpoons Fe^{\bullet IV\bullet}R^+ \text{ (unstable)}^{7b}$$

$$5/5' \quad Fe^{III}R + e^- \rightleftharpoons Fe^{II}R^- \text{ (stable)}$$

$$6 \quad Fe^{II}R^- + e^- \rightleftharpoons Fe^{\bullet I\bullet}R^{2-} \text{ (moderately stable)}^{7c}$$

Figure 1d shows the transformation of the preceding cyclic voltammogram upon addition of CO as a function of scan rate. Upon oxidation of $Fe^{II}Et^-$ into $Fe^{III}R$, insertion occurs, giving rise to a new reversible wave (8/8') corresponding to the $Fe^{III}COEt/Fe^{II}COEt^-$ couple. The production of $Fe^{II}COEt^-$ is the more efficient the lower the scan rate, pointing to the following electrocatalytic (chain) mechanism:

$$Fe^{II}R^- - e^- \rightleftharpoons Fe^{III}R \qquad (1)$$

$$Fe^{III}R + CO \xrightarrow{k_2} Fe^{III}COR \qquad (2)^{8a}$$

$$Fe^{III}COR + Fe^{II}R^- \rightarrow Fe^{II}COR^- + Fe^{III}R \qquad (3)^{8b,c}$$

At the same time, another reversible wave appears upon scan reversal located at the same potential as the Fe(II)/Fe(I) wave (2/2') in the presence of CO (see Figure 1b). This indicates that the insertion reaction (2) is not complete but competes with the cleavage of the iron–carbon bond in agreement with previous observation.[3b] As shown earlier,[2a-d] $Fe^{III}R$ porphyrins are less stable than $Fe^{II}R^-$ porphyrins toward R• radical cleavage. With primary alkyls, $Fe^{III}R$ complexes are however stable within the time scale of cyclic voltammetry and even of preparative-scale electrolysis. Their decomposition, in the present case, is facilitated by the presence of CO, which stabilizes the resulting iron(II) complex:

$$Fe^{III}R + CO \xrightarrow{k_4} Fe^{II}CO + R^\bullet \qquad (4)^{8a}$$

The outcome of the competition between reactions 2 and 4 can be quantitatively estimated by preparative-scale oxidation at −0.6

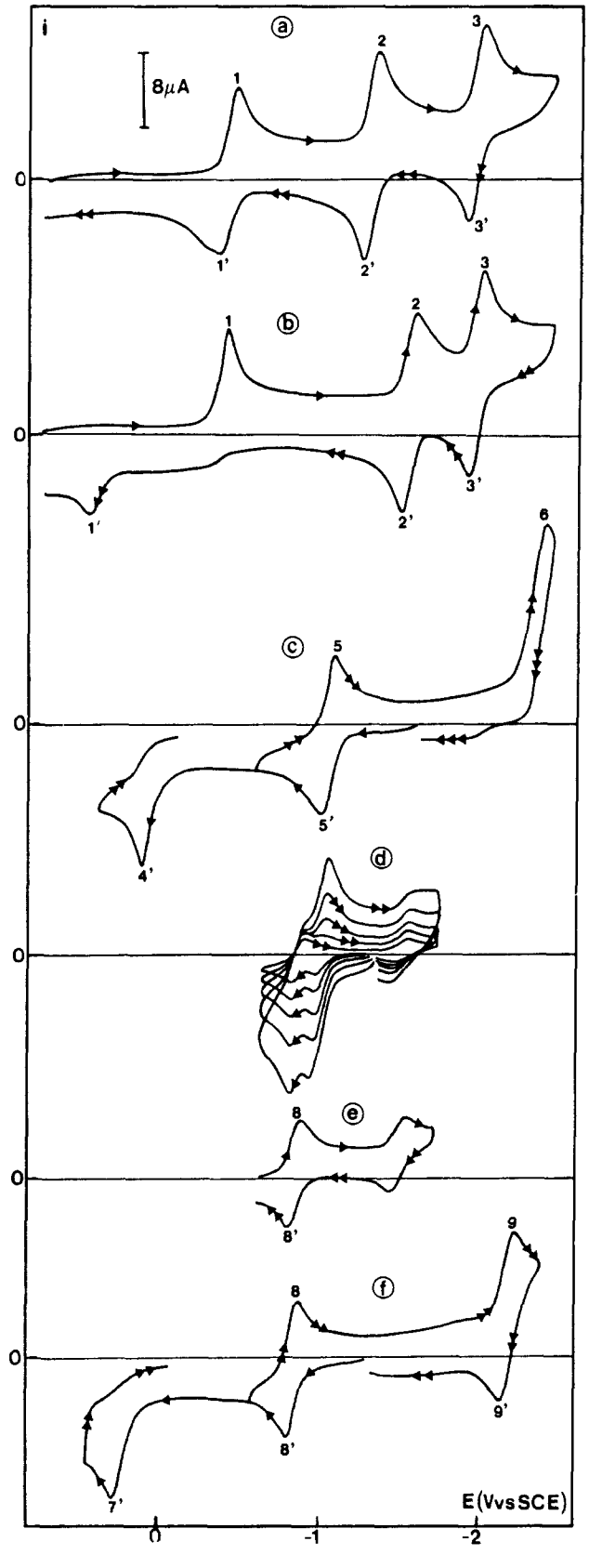

Figure 1. Cyclic voltammetric investigation of CO insertion in the C–Fe bond of σ-EtFeOEP (in DMF + 0.1 M NEt_4ClO_4, at 20 °C, scan rate 0.1 V s^{-1} unless otherwise stated). (a) (OEP)FeCl (1 mM). (b) (OEP)FeCl in the presence of CO (1 atm). (c) (OEP)FeEt (1 mM) obtained from electrolysis of (OEP)FeCl at −1.6 V vs SCE in the presence of 2 mM EtBr, followed by removal of excess EtBr. (d) Addition of CO (1 atm) to the preceding solution. Scan rate: 0.02, 0.05, 0.10, 0.20, 0.40 V s^{-1}. (e) After electrolysis of the solution in (c) at wave 5' (−0.6 V vs SCE) in the presence of CO (1 atm). (f) Cyclic voltammetry of pure (OEP)FeCOEt (1 mM) obtained as described in the text.

(6) (a) A detailed investigation of CO binding to iron(I) porphyrins has been carried out previously.[6b] It has been shown to be enhanced by strong axial ligands and by the presence of secondary amide groups in the vicinity of the porphyrin ring. With OEP and DMF as axial ligand, CO binding to Fe(I) is negligible. (b) Croisy, A.; Lexa, D.; Momenteau, M.; Savéant, J.-M. *Organometallics* **1985**, *4*, 1574.

(7) (a) Note that the numbering of the waves is different from that used in ref 3a. (b) Reversibility of wave 4' is obtained at −50 °C where the stability of the $Fe^{\bullet IV\bullet}Et^+$ complex is sufficient for its reduction to be observed at 0.1 V s^{-1}.[2d] (c) The wave becomes reversible at 1 V s^{-1}.

(8) (a) As shown previously,[3b] reactions 2 and 4 are first order in CO and $Fe^{III}R$. (b) The reduction of $Fe^{III}COR$ to $Fe^{II}COR^-$ could also occur, at least in principle, at the electrode surface. However since reaction 2 is slow, $Fe^{III}COR$ is formed far from the electrode surface and is thus predominantly reduced in solution according to reaction 3 before having time to diffuse back to the electrode surface and be reduced there.[8c] (c) Andrieux, C. P.; Savéant, J.-M. Electrochemical Reactions. In *Investigations of Rates and Mechanisms of Reactions, Techniques of Chemistry*, 4th ed.; Bernasconi, C. F., Ed.; Wiley: New York, 1986; Vol. 6, Part 2, pp 305–390.

Table I. UV–vis Spectral Characteristics of σ-Ethyl- and σ-Propionyliron Octaethylporphyrins [λ (nm) ε (M^{-1} cm^{-1})][a]

$Fe^{II}R^-$	353 (7.2 × 10^4), 418 (7.7 × 10^4), 543 (2.8 × 10^4), 708 (0.3 × 10^4)
$Fe^{II}COR^-$	341 (4.6 × 10^4), 403 (7.8 × 10^4), 506 (1.0 × 10^4), 538 (3.2 × 10^4), 711 (0.3 × 10^4)
$Fe^{III}R$	392 (10 × 10^4), 520 × (sh), 555 (1.6 × 10^4)
$Fe^{III}COR$	385 (10.1 × 10^4), 514 × (sh), 545 (1.5 × 10^4)

[a] In DMF + 0.1 M NEt_4ClO_4.

V vs SCE. As shown in Figure 1e, both $Fe^{III}COR$ and $Fe^{II}CO$ are obtained. The ratio of the heights of waves 8/8′ and 2/2′ provides the value of k_2/k_4. A value of 1.5 is found in the present case.

As seen in Figure 1d, both reactions 2 and 4 are not very rapid. Full reversibility of wave 5/5′ is obtained at about 1 V s^{-1}, showing that k_2 and k_4 are of the order of 5 s^{-1} [8c] in terms of pseudo-first-order rate constants, i.e., 5 atm^{-1} s^{-1} in terms of second-order rate constants. At this scan rate, the standard potential of the $Fe^{III}R/Fe^{II}R^-$ couple (wave 5/5′) is -0.97_0 V vs SCE, i.e., 25 mV positive to that of the same couple in the absence of CO (Figure 1c). This results from the binding of CO to the $Fe^{II}R^-$ complex with an association constant of 1.8 atm^{-1} (6.8 × 10^2 M^{-1}).[9]

Figure 1f shows the cyclic voltammogram of a pure solution of the $Fe^{II}COR^-$ complex. This was obtained as follows. A small amount of EtBr (2 mM) was added to the solution corresponding to Figure 1e, and the resulting solution was electrolyzed at a potential slightly negative to wave 2/2′ (−1.75 V vs SCE), thus converting the iron porphyrin regenerated from the reaction with CO to the corresponding $Fe^{II}R^-$ complex. Another electrolysis was then performed at a potential slightly positive to wave 5/5′ (−0.95 V vs SCE). Of the $Fe^{II}R$ complex 60% was thus converted to $Fe^{II}COR^-$ and 40% to $Fe^{II}CO$. Repeating these operations five times led to a practically pure solution of $Fe^{II}COR^-$.

Like the σ-alkyl porphyrins, the σ-acyl porphyrins show three waves (Figure 1f): two reversible waves (8/8′ and 9/9′) corresponding to the $Fe^{III}COR/Fe^{II}COR^-$ and $Fe^{II}COR^-/Fe^{I}COR^{2-}$ couples, respectively, and an irreversible wave (7′) corresponding to the one-electron oxidation of $Fe^{III}COR$ to an unstable $Fe^{IV}COR^+$ complex. The waves of the acyl complex are all positive to the waves of the parent alkyl complex as expected from the electron-withdrawing character of the COR group as compared to the R group.

The preceding results are confirmed by thin-layer spectroelectrochemistry. The $Fe^{II}R^-$ complex was prepared in situ from $(OEP)Fe^{III}Cl$ by setting the working electrode potential at a value slightly negative to the Fe(I)/Fe("0") wave (−2.05 V vs SCE) under 1 atm of CO, in the presence of a small amount of EtBr (0.3 mM) so as to generate $Fe^{II}R^-$ directly from $Fe("0")^{2-}$ and thus to avoid the reaction with $Fe(I)^-$ that would produce $Fe^{III}R$ at least transitorily. As seen in Figure 2, a mixture of two complexes is obtained. The bands noted 1 are those of the $Fe^{II}R^-$ complex as checked with a pure sample independently prepared (Table I). The bands noted 2 are attributed to the complex resulting from the binding of CO to $Fe^{II}R^-$, as a sixth ligand, i.e., without insertion. From the association constant derived above from the cyclic voltammetric data (1.8 atm^{-1}), the proportions of $Fe^{II}R^-$ and $OCFe^{II}R^-$ are 36% and 64%, respectively, thus leading to the following ε-values for the latter complex [λ (nm) (ε (M^{-1} cm^{-1}))]: 385 (6.7 × 10^4), 491 (4.4 × 10^4), 544 (0.9 × 10^4). Upon reoxidation at −0.95V, i.e., slightly positive to the peak of wave 5′, a new spectrum appears (Figure 2) that can be attributed to a mixture of the $Fe^{II}COR^-$ insertion complex and $Fe^{II}CO$. The bands attributed to the former complex are the same as that obtained (see Table I) from thin-layer spectroelectrochemistry of $(OEP)Fe^{III}Cl$ at the potential of formation of $Fe(I)^-$ in the presence of CO and EtBr, i.e., the same procedure as previously employed with *n*-hexyl bromide.[3a] The spectra are pratically the same in both cases. Since the acyl complex has been

(9) (a) Taking 2.65 M atm^{-1} as the solubility of CO in DMF.[15b] (b) Jameson, G. B.; Ibers, I. A. *Comments Inorg. Chem.* **1983**, *2*, 97.

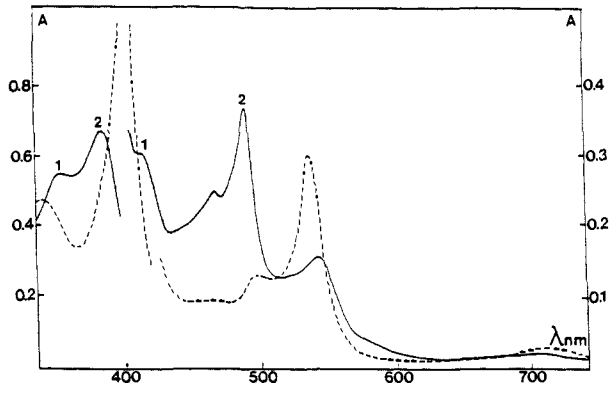

Figure 2. Spectroelectrochemistry of $(OEP)Fe^{III}Cl$ (0.2 mM), in DMF + 0.1 M NEt_4ClO_4, in the presence of 1 atm of CO and of 0.3 mM EtBr: solid line, electrolysis at −2.05 V vs SCE; dashed line, reoxidation at −0.95 V vs SCE. The bands noted 1 are those of $Fe^{II}R^-$, and the bands noted 2 are those of its CO complex.

identified by its IR and ^{13}C NMR characteristics in the *n*-hexyl case, we can infer that the acyl complex was also obtained in the present case.

The spectra of the acyl complex ressemble that of parent alkyl complex at both oxidation states, the bands being, however, shifted toward shorter wavelengths for the same reason that the redox potentials are shifted positively. The above described step-by-step electrolyses followed by either cyclic voltammetric or UV–vis spectroscopic characterization were useful for investigating the reaction mechanism. However, the most convenient way for preparing the acyl complex is to carry out an electrolysis of $(OEP)Fe^{III}Cl$ at the potential where Fe(I) is generated (−1.7 V vs SCE) in the presence of a large excess of the alkyl halide (e.g., 10 mM for 1 mM porphyrin) under 1 atm of CO. The $Fe^{II}COR^-$ complex is thus obtained quantitatively. This is because the primary product of the reaction of $Fe(I)^-$ with the alkyl halide is the $Fe^{III}R$ complex,[2c] which is able to undergo CO insertion in contrast to the $Fe^{II}R^-$ complex. The $Fe^{II}COR^-$ complex is then generated by means of a chain process (reactions 2 and 3). The presence of a large excess of the alkyl halide then helps to minimize the competing reduction of $Fe^{III}R$ by $Fe(I)^-$ by decreasing the concentration of the latter species. A portion of the $Fe^{III}R$ complex (40%) is concurrently converted into the $Fe^{II}CO$ complex, but this is further reduced to $Fe(I)^-$, which reacts with the excess alkyl halide, thus starting a new catalytic cycle.

At this point, we can conclude that σ-ethyliron octaethylporphyrin as well as higher primary complexes undergo CO insertion at the iron(III) oxidation level, leading to the corresponding acyl complex. Under 1 atm of CO the reaction is rather slow, with a rate constant of the order of 5 s^{-1} atm^{-1}, and competes with decomposition of the alkyl complex into $Fe^{II}CO$ in a 3:2 ratio.

What happens with other alkyl groups is the purpose of the following discussion, starting with *methyl*. It is interesting to compare the case of methyl to that of longer linear alkyl groups, since with nonmacrocyclic complexes insertion of CO has been shown to be slower in the first case than in the second.[4] The same is observed in the present case as results from the following set of experiments.

$Fe^{II}CH_3^-$ was prepared by electrolysis of $(OEP)Fe^{III}Cl$ at −1.6 V vs SCE (corresponding to the generation of $Fe(I)^-$) under 1 atm of CH_3Cl. The voltammogram of the resulting solution is similar to what was obtained in the case of ethyl (Figure 3a).

When CO (1 atm) is introduced into the solution, the voltammogram shown in Figure 3b results. It is seen that CO insertion does not occur within the cyclic voltammetric time scale at 0.1 V s^{-1}; wave 5/5′ remains reversible and is merely shifted positively as a result of the binding of CO to $Fe^{II}CH_3^-$, but no wave corresponding to the formation of $Fe^{II}COCH_3^-$ appears. Wave 4′ is slightly shifted negatively, indicating that the decomposition of the $Fe^{IV}R^+$ complex is accelerated by the presence of CO. CO insertion does not occur even at a scan rate as low as 0.02 V s^{-1}. Decomposition of $Fe^{III}CH_3$ into $Fe^{II}CO$ does not occur

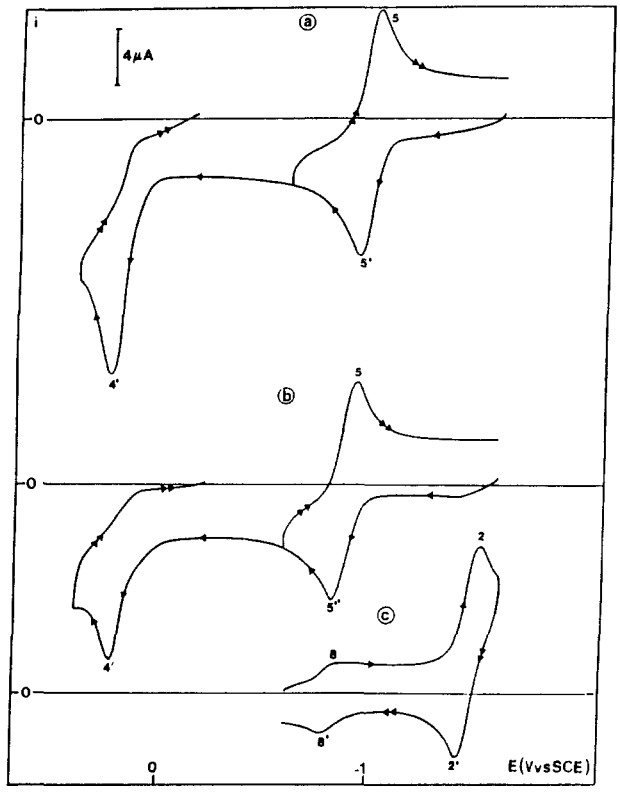

Figure 3. Cyclic voltammetric investigation of the reaction of CO with σ-MeFeOEP (in DMF + 0.1 M NEt_4ClO_4 at 20 °C, scan rate 0.1 V s^{-1}). (a) $Fe^{II}CH_3^-$ prepared from electrolysis of (OEP)$Fe^{III}Cl$ (1 mM) at −1.6 V vs SCE (generation of $Fe(I)^-$) under 1 atm of CH_3Cl. (b) Same solution as in (a) under 1 atm of CO. (c) Same solution as in (b) after reoxidation at −0.6 V vs SCE.

either, at this scan rate. If CO is removed by bubbling argon through the solution, the voltammogram shown in Figure 3a is restored, showing that no irreversible transformation of the starting $Fe^{II}CH_3^-$ complex has occurred. $Fe^{III}CH_3$ thus appears as more stable than the other primary σ-alkyl complexes vis-à-vis both insertion and decomposition. These two reactions, however, take place at preparative scale; oxidation at −0.6 V vs SCE produces a 10:90 mixture of $Fe^{III}COCH_3$ and $Fe^{II}CO$.

These results are confirmed by thin-layer spectroelectrochemistry. Figure 4a shows the spectrum of the $Fe^{II}CH_3^-$ complex obtained from reduction of (OEP)$Fe^{III}Cl$ either at −1.5 V vs SCE in the presence of a large excess of CH_3Cl (1 atm) or at −2.05 V vs SCE in the presence of a small excess of CH_3Cl [λ (nm) (ε (M^{-1} cm^{-1})]: 350 (6.4 × 10^4), 416 (6.1 × 10^4), 544 (2.9 × 10^4). When the latter experiment is carried out in the presence of 1 atm of CO, the spectrum shown in Figure 4b ensues. It shows the formation of a mixture of $OCFe^{II}CH_3^-$ and $Fe^{II}CH_3^-$ in a 93:7 ratio as estimated from the equilibrium constant (14.4 atm^{-1}) calculated from the potential shift of wave 5/5′ described earlier. The following UV–vis spectral characteristics of the $OCFe^{II}CH_3^-$ ensues [λ (nm) (ε (M^{-1} cm^{-1}))]: 375 (5.8 × 10^4), 478 (5.4 × 10^4), 542 (0.7 × 10^4).

The IR characteristics of this complex were also investigated: the CO band wavenumber was found to be 1886 cm^{-1}, the lowest value ever found for an $Fe^{II}CO$–porphyrin complex,[10] thus indicating considerable electron transfer from the carbanionic ligand to the CO moiety.

Back to UV–vis spectroelectrochemistry, reoxidation at −0.6V vs SCE produces a mixture of the acyl complex, $Fe^{III}COCH_3$, and

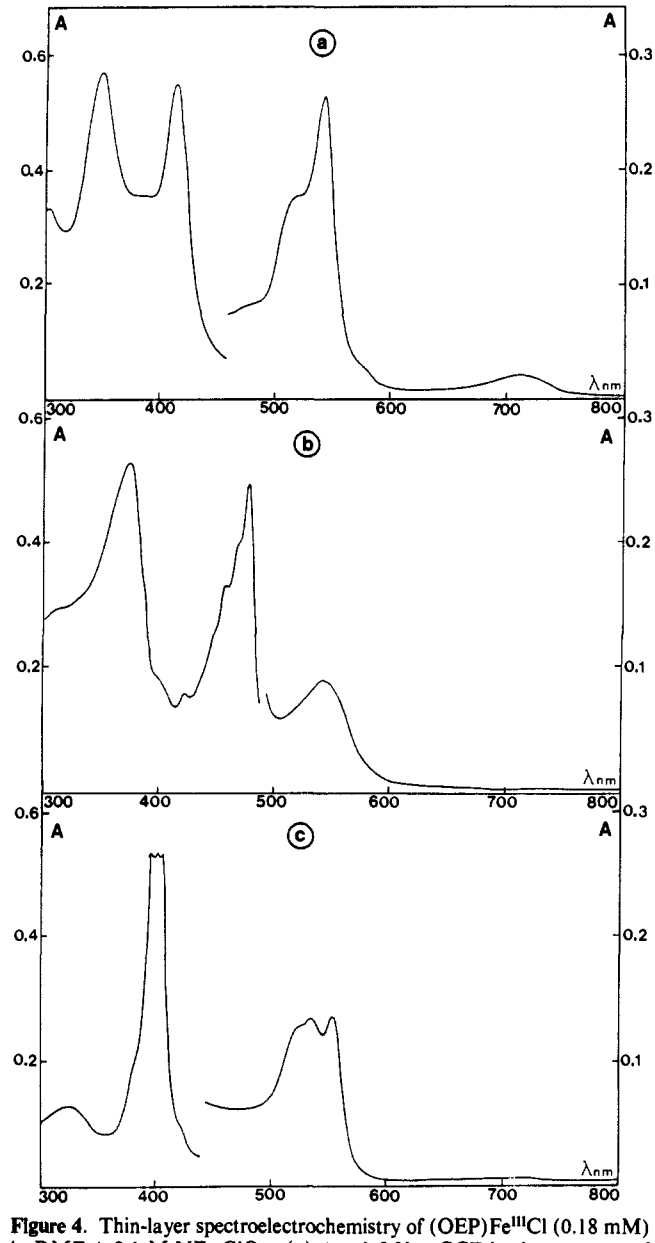

Figure 4. Thin-layer spectroelectrochemistry of (OEP)$Fe^{III}Cl$ (0.18 mM) in DMF + 0.1 M NEt_4ClO_4. (a) At −1.5 V vs SCE in the presence of a large excess of CH_3Cl (1 atm) or at −2.05 V vs SCE in the presence of a small excess of CH_3Cl. (b) Same as the latter experiment of (a), in the presence of 1 atm of CO. (c) Same as (b) after reoxidation at −0.6 V vs SCE and then −1 V vs SCE.

$Fe^{II}CO$. After reduction of $Fe^{III}COCH_3$, at −1.0 V vs SCE, a 10:90 mixture of $Fe^{II}COCH_3^-$ and $Fe^{II}CO$ is obtained (Figure 4c). The $Fe^{II}COCH_3^-$ complex was identified and titrated by comparison with the product obtained from the reaction of acetic anhydride with (OEP)$Fe^{*0*\,2-}$.[5]

It can thus be concluded that CO insertion in the iron–methyl carbon bond does occur at the iron(III) oxidation state. It is however slower and less favorable, as compared to the CO-induced decomposition of $Fe^{III}R$, than in the case of other primary σ-alkyl complexes.

The situation encountered with *tert*-butyl is quite different from the cases examined so far. As shown earlier[2d] the σ-*tert*-butyliron(III) complex is unstable on the time scale of preparative electrolysis and even of thin-layer spectroelectrochemistry. In cyclic voltammetry the 5′/5 wave is reversible only above 0.4 V s^{-1} (Figure 5a). Since, on the other hand, the CO–*tert*-butyl radical is itself quite unstable, yielding CO and *t*-Bu*,[11] there is

(10) (a) The differential spectrum of $Fe^{II}CH_3^-$ in the presence of CO (1 atm) toward in its absence shows a CO vibration band at 1886 cm^{-1} (in DMF + 0.1 M NEt_4ClO_4). This wavenumber value is considerably lower than that of (OEP)$Fe^{II}CO$ in the same solvent[10b] and even those of either (OEP)$Fe^{II}CO$ thiolate[10c] or α-PFFe$^{II}CO^-$ (Figure 7).[10d] (b) 1940 cm^{-1} (this work), 1948 cm^{-1} (in pure DMF).[10c] (c) 1923 cm^{-1}: Ogoshi, H.; Sugimoto, H.; Yoshida, Z. *Bull. Chem. Soc. Jpn.* **1978**, *51*, 2369. (d) 1931 cm^{-1}.[6b]

(11) Abell, P. J. In *Free Radicals*; Kochi, J. K., Ed.; Wiley: New York, 1973; p 94.

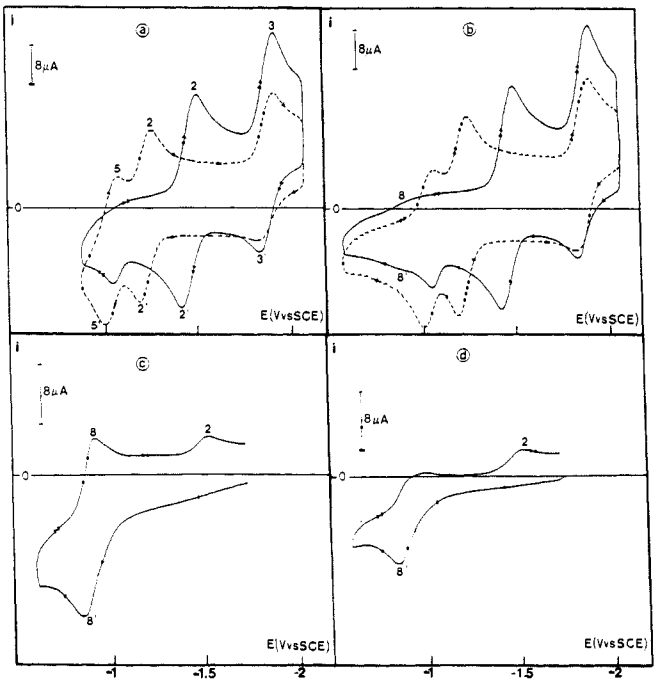

Figure 5. (a, b) Cyclic voltammetry of (OEP)$Fe^{III}Cl$ (1 mM) in DMF + 0.1 M NEt_4ClO_4 in the presence of *t*-BuCl (180 mM) at 0.4 V s^{-1}, showing that wave 5/5′ becomes irreversible upon addition of CO (a) and the appearance of (OEP)$Fe^{II}CO$-*t*-Bu (8/8′). (b) Solid line: in the presence of 1 atm of CO. Dashed line: without CO. (c, d) Cyclic voltammetry of the solution obtained electrolysis of (OEP)$Fe^{III}Cl$ (0.8 mM) at −1.9 V vs SCE in the presence of 70 mM *t*-BuCl and 1 atm of CO. Scan rates: 0.4 V s^{-1} (c) and 0.1 V s^{-1} (d).

little chance that insertion of CO could occur at the *σ-tert*-butyliron(III) oxidation level. Insertion is however possible, but at the *σ-tert*-butyliron(II) oxidation level as results from the following experiments.

In the presence of *t*-BuCl, $Fe(I)^-$ does not react on the time scale of cyclic voltammetry, but $Fe("0")^{2-}$ gives rise to the 5/5′ wave, characteristic of the $Fe^{III}R/Fe^{II}R^-$ couple (Figure 5a). In the presence of CO, besides the negative shift of the 2/2′ wave due to the binding of CO to Fe(II), we note that wave 5/5′ becomes irreversible (Figure 5a) and that a small amount of $Fe^{II}CO$-*t*-Bu is formed, revealed by the 8/8′ wave (Figure 5b). Since Fe^{III}-*t*-Bu has not been formed under these conditions, this shows that insertion takes place in the Fe^{II}-*t*-Bu^- complex. Quantitative formation of the $Fe^{II}CO$-*t*-Bu^- complex is obtained upon electrolysis at −1.9 V vs SCE (a potential where $Fe("0")^{2-}$ is formed) as seen in Figure 5c. CO insertion in the Fe^{II}-*t*-Bu^- complex may be accompanied by the same decomposition. If this occurs, the resulting complex is reduced into its $Fe("0")^{2-}$ form, which reacts with *t*-BuCl, yielding Fe(II)-*t*-Bu^- in which insertion can de novo take place. We note that $Fe^{III}CO$-*t*-Bu is not very stable (wave 8/8′ is reversible at 0.4 V s^{-1} (Figure 5c) but not quite at 0.1 V s^{-1} (Figure 5d)) and that its decomposition regenerates the Fe^{III}-*t*-Bu complex.

The formation of the $Fe^{II}CO$-*t*-Bu^- complex is also observed in thin-layer spectroelectrochemistry: upon reduction at −1.9 V vs SCE, a spectrum similar to those observed with the other acyls is obtained.

The case of *benzyl* is also different from that of all other alkyls. While the $Fe^{III}R$ and $Fe^{II}R^-$ complexes can be easily obtained from the reaction of $Fe(I)^-$ or $Fe("0")^{2-}$ with $PhCH_2Br$ or $PhCH_2Cl$, introduction of CO decomposes these complexes with no formation of insertion products.

The behavior of *σ-aryl* complexes is another interesting case since migratory insertion of CO has been shown to be much slower compared to alkyl complexes.[12] Starting, this time from the

(12) Cawse, J. N.; Fiato, R. A.; Pruet, R. I. *J. Organomet. Chem.* **1979**, *172*, 405.

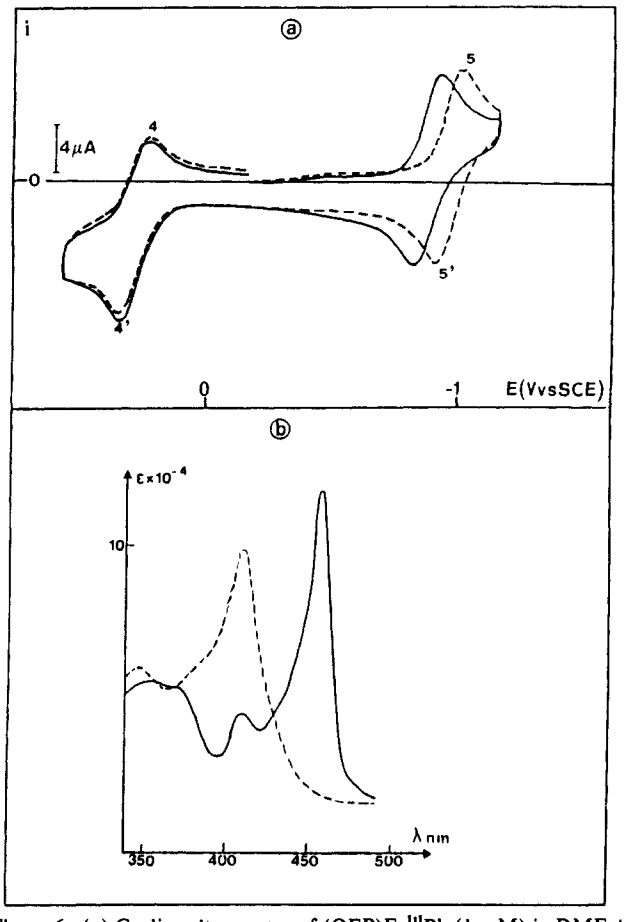

Figure 6. (a) Cyclic voltammetry of (OEP)$Fe^{III}Ph$ (1 mM) in DMF + 0.1 M NEt_4ClO_4 in the absence (dashed line) and presence (solid line, 1 atm) of CO. (b) Thin-layer spectroelectrochemistry of (OEP)$Fe^{III}Ph$ (0.2 mM) in DMF + 0.1 M NEt_4ClO_4 in the absence (dashed line) and presence of CO (1 atm) (solid line).

Table II. Standard Potentials[a] of the $Fe^{III}CO$-*n*-Hex/$Fe^{II}CO$-*n*-Hex^- and Fe^{III}-*n*-Hex/Fe^{II}-*n*-Hex^- Couples in DMF + 0.1 M NEt_4ClO_4 as a Function of the Porphyrin Structure (Figure 7)

porphyrin	$Fe^{III}CO$-*n*-Hex/ $Fe^{II}CO$-*n*-Hex^-	Fe^{III}-*n*-Hex/ Fe^{II}-*n*-Hex^-
OEP	-0.83_0	-0.99_5
TPP	-0.60_0	-0.74_5
e-$(C_{12})_2$-CT	-0.78_0	-0.95_0
a-$(C_{12})_2$-CT	-0.45_0	-0.58_5
a-PF	-0.43_0	-0.56_0

[a] In volts vs SCE.

(OEP)$Fe^{III}Ph$ complex prepared from the reaction of (OEP)$Fe^{III}Cl$ with phenylhydrazine,[13] introduction of 1 atm of CO in a DMF solution did not result in any noticeable insertion after 2 h[14] as checked by cyclic voltammetry and UV–vis spectrometry.

Cyclic voltammetry shows (Figure 6a) a positive shift of the $Fe^{III}Ph/Fe^{II}Ph^-$ wave (5/5′) with the addition of CO, while the $Fe^{III}Ph/Fe^{\cdot IV}Ph^+$ wave (4/4′) remains unaffected,[15] indicating that CO binds to $Fe^{II}Ph^-$ and not to $Fe^{III}Ph$. This is confirmed by UV–vis spectroscopy (Figure 6b): the Soret band of (OEP)$Fe^{II}Ph^-$ obtained upon electrolysis at −1.0 V vs SCE is quite significantly shifted toward longer wavelength upon introduction of CO. Spectral analysis of the mixture of $Fe^{II}Ph^-$ and $OCFe^{II}Ph^-$

(13) Battioni, P.; Mahy, J. P.; Gillet, G.; Mansuy, D. *J. Am. Chem. Soc.* **1983**, *105*, 1399.

(14) After 4 h, a slight decomposition to the $Fe^{II}CO$ complex begins to appear.

(15) (a) $Fe^{\cdot IV}Ph^+$ appears stable in the time scale of cyclic voltammetry at 0.1 V s^{-1}. At longer times, Ph^+ migration to a porphyrin nitrogen occurs.[15b] (b) Lançon, D.; Cocolios, P.; Guilard, R.; Kadish, K. M. *J. Am. Chem. Soc.* **1984**, *106*, 4472.

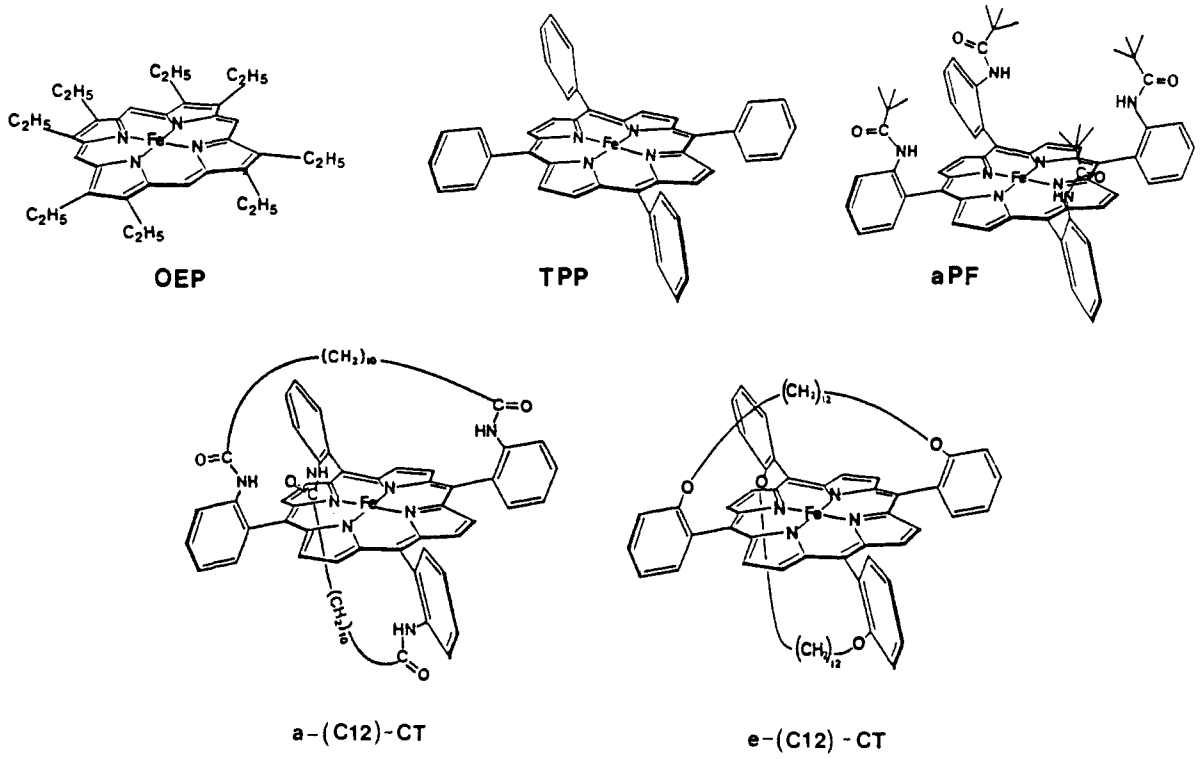

Figure 7. Porphyrins investigated in this work.

thus obtained gave a value of the association constant of 18.5 atm^{-1} (7×10^3 M^{-1}) in agreement with the peak potential shift (80 mV) observed in cyclic voltammetry.

Several other porphyrins (those shown in Figure 7) were also briefly investigated. CO insertion in the Fe(III)–C bond was shown to occur in all cases in the case of the *n*-hexyl complexes. The standard potentials of the $Fe^{III}COR/Fe^{II}COR^-$ couple are listed in Table II together with those of the parent $Fe^{III}R/Fe^{II}R^-$ couple. As with OEP, the former couple is positive to the latter in all cases. Inductive effects are of the same type for both complexes: the presence of electron-donating groups render the standard potential more negative. Through-space interaction of the NHCO groups in basket-handle porphyrins results in a stabilization of the negatively charged iron(II) complexes in acyl as well as in alkyl complexes.[2b,d] This has been shown to occur with many other reactions, electron transfers, or ligand exchanges involving an increase of the negative charge.[16]

Experimental Section

Chemicals. Fe^{III}(TPP)Cl and Fe^{III}(OEP)Cl were from commercial origin and were used as received. The other porphyrins were synthesized and characterized as already described: *e*-$(C_{12})_2$-CT,[17a] *a*-$(C_{12})_2$-CT,[17b] *a*-PF.[17c] DMF and alkyl halides were distilled before use. NEt_4ClO_4 (Fluka purum) was used as supporting electrolyte. It was recrystallized three times before use in a 1:2 ethyl acetate–ethanol mixture.

Cyclic Voltammetry and Thin-Layer UV–vis Spectroelectrochemistry. The cell and instrumentation were the same as previously described.[18] The solutions were degassed by argon (U grade) or CO (N47 grade). For cyclic voltammetry experiments, the working electrode was a 3-mm-diameter glassy carbon disk, and for thin-layer UV–vis spectroelectrochemistry, a platinum grid. In the latter, the optical length was 0.05 cm. All potentials are referred to the NaCl aqueous saturated calomel electrode (SCE).

Preparative Electrolyses. The instrumentation was the same as previously described.[2a] The cell consisted of a thermostated (at 20 °C) water-jacketed vessel made air-tight by a septum. The electrodes were introduced in the cell by four outlets through the septum. Four electrodes were used in order to record in situ cyclic voltammograms,[19] during preparative electrolysis: two working electrodes, used alternatively, one reference electrode (Cd(Hg)/$CdCl_2$ (saturated solution in DMF)),[20] and one auxiliary electrode (platinum grid). These two latter electrodes were separated from the solution by means of a fritted glass and were used both for electrolysis and cyclic voltammetry. For cyclic voltammetric recordings, the working electrode was the same as above. The working electrode used for electrolysis was a large (7 cm^2) carbon half-crucible. The cell was degassed by an argon stream for 30 min before the degassed porphyrin solution was introduced.

IR Spectroscopy. After preparative electrolysis, the $Fe^{II}CH_3^-$ or $OCFe^{II}CH_3^-$ solutions were transferred in a degassed IR cell under an argon or CO stream, respectively. The IR spectra were recorded on a Fourier transform apparatus (Nicolet 5MX) in a 0.1-mm KBr cell.

Conclusions

Carbon monoxide inserts in the carbon–iron bond of σ-alkyliron porphyrins with the exception of benzyl complexes. CO insertion does not occur in σ-aryl complexes. With methyl and other primary alkyls, insertion takes place at the $Fe^{III}R$ oxidation state rather than at the $Fe^{II}R^-$ state, although CO binds to the latter complex. The insertion of CO in the Fe(III)–C bond is accompanied by decomposition of the alkyl complex, this being enhanced by the binding of CO to the resulting Fe(II) complex. The opposite is true for the *tert*-butyl derivative: insertion does not occur in the $Fe^{III}R$ complex but rather in the $Fe^{II}R^-$ complex. CO insertion thus appears to result from the balance between three factors, stability of the Fe–C bond toward homolysis, stability of the $^{\bullet}COR$

(16) (a) Gueutin, C.; Lexa, D.; Momenteau, M.; Savéant, J.-M.; Xu, F. *Inorg. Chem.* **1986**, *25*, 4294. (b) Lexa, D.; Savéant, J.-M. In *Redox Chemistry and Interfacial Behavior of Biological Molecules*; Dryhurst, G., Niki, K., Eds.; Plenum Press: New York, 1988; pp 1–26.

(17) (a) Momenteau, M.; Mispelter, J.; Loock, B.; Bisagni, E. *J. Chem. Soc., Perkin Trans. I* **1983**, 189. (b) Momenteau, M.; Mispelter, J.; Loock, B.; Lhoste, J. M. *J. Chem. Soc., Perkin Trans. I* **1985**, 221. (c) Collman, J. P.; Gagne, R. R.; Reed, C. A.; Malbert, T. R.; Lang, G.; Robinson, W. T. *J. Am. Chem. Soc.* **1975**, *97*, 1427.

(18) Lexa, D.; Savéant, J.-M.; Zickler, J. *J. Am. Chem. Soc.* **1977**, *99*, 2786.

(19) (a) Cyclic voltammograms of complexes prepared by electrolysis can be recorded either after the transfer of the electrolyzed solution from the preparative electrolysis cell to a voltammetric cell (under argon or CO pressure) or, without transfer, in the preparative electrolysis cell. The latter procedure has the advantage of eliminating a possible contamination of the solution by air dioxygen during the transfer. As a matter of fact, the σ-acyliron porphyrins[19b] are unstable in the presence of oxygen. (b) In the presence of oxygen, the (OEP)Fe^{III}COR complexes produces to the corresponding μ-oxo dimer as in the case of (OEP)Fe^{III}R complexes.[19c,d] (c) Ogoshi, H.; Sugimoto, H.; Yoshida, Z.; Kobayashi, H.; Sakai, H.; Maeda, Y. *J. Organomet. Chem.* **1982**, *234*, 185. (d) Arasasingham, R. D.; Balch, A. L.; Latos-Grazynky, L. *J. Am. Chem. Soc.* **1987**, *109*, 5846.

(20) Marple, L. W. *Anal. Chem.* **1967**, *39*, 86.

radical toward decomposition into CO and R•, and strength of the Fe–COR bond, even if these steps occur concertedly. CO insertion does not occur in the case of phenyl and is slower in the case of methyl as compared to the other primary alkyls because the Fe(III)–C bond is stronger in the first two cases than in the others. The facile decomposition of the •COR radical into CO and R• prevents CO insertion in the Fe(III)–C bond in the case of benzyl and *tert*-butyl. The acyl radical has an electrophilic character that is less pronounced in the case of methyl than the other alkyls, resulting in a poorer insertion to decomposition ratio in the former case than in the latter. The electrophilic character of the •COR radical is also presumably involved in the insertion of CO in the Fe(II)–C bond in the case of *tert*-butyl (combination of •COR with $Fe(I)^-$) in spite of the tendency of the •CO-*t*-Bu radical to decompose into CO and *t*-Bu•.

Acknowledgment. We are indebted to A. Croisy, J. Mispelter, and C. Schaeffer for helpful discussions on the IR and NMR data.

Proton Abstraction from Dimethyl(2-substituted-9-fluorenyl)sulfonium Ions. Evidence for Changes in Transition-State Structure[1]

Christopher J. Murray and William P. Jencks*

Contribution No. 1699 from the Graduate Department of Biochemistry, Brandeis University, Waltham, Massachusetts 02254-9110. *Received July 24, 1989*

Abstract: Rate and equilibrium constants for C(9)-^{1}H, -^{2}H, and -^{3}H abstraction from dimethyl(2-substituted-9-fluorenyl)sulfonium tetrafluoroborates (**1a**, X = H; **1b**, X = Br; **1c**, X = NO_2) catalyzed by oxygen and amine bases have been determined by ^{1}H NMR and detritiation in 95% L_2O–5% Me_2SO (v:v) at 28 °C and ionic strength 1.0 M (KCl). The pK_a values are **1a**, 13.7, **1b**, 12.4, and **1c**, 10.6. Rate constants at $\Delta pK = 0$ are $\sim 10^4$ M^{-1} s^{-1}. The modest intrinsic barrier for proton abstraction from **1** is similar to that for the corresponding cyano-activated fluorenes and is attributed to resonance delocalization into the fluorene ring, with little contribution from solvent reorganization. The primary kinetic isotope effects decrease with increasing ΔpK, but do not approach unity even for $\Delta pK > 15$. The secondary solvent isotope effect of $k_{H_2O}/k_{D_2O} = 2.3$ for ^{3}H transfer from **1a** to water and the absence of strong inhibition of ^{1}H and ^{3}H exchange by D_3O^+ show that proton transfer to water is direct. The secondary solvent lyoxide isotope effects of $k_{OD}/k_{OH} = 2.0$ for ^{3}H exchange of **1a** and **1b** are close to the limiting isotope effect of $K_{OD}/K_{OH} = 2.4$ at equilibrium. Brønsted α values for proton exchange from **1a–c** decrease with increasing pK_a^{BH} from 0.97 to 0.59 for a series of oxygen anion catalysts and from 0.67 to 0.46 for amine catalysts that span a reactivity range of $>10^5$. The Brønsted β values for catalysis by substituted acetate ions decrease with decreasing pK_a^{CH} from 0.98 to 0.75 and 0.75 to 0.70 for catalysis by amines. These changes are described by the interaction coefficient $p_{xy} = \partial\beta/\partial pK_a^{CH} = \partial\alpha/-\partial pK_a^{BH} = 0.04$–$0.08$. It is concluded that these changes represent changes in transition-state structure that are related to the large intrinsic reactivity of these carbon acids.

We are concerned here with changes in transition-state structure that are manifested by changes in the slopes of structure–reeactivity relationships for proton-transfer reactions.[2-5] Changes in slope that produce curvature in a Brønsted plot have been demonstrated for several proton transfers to and from carbon, including the ionization of acetylacetone[6] and the protonation of diazoacetate anions.[7] There is also precedent for changes in Brønsted slopes with a common set of catalysts for enolization of a series of ketones, keto esters, and diketones,[2,8] for ionization of (4-nitroaryl)-acetonitriles,[9] and for protonation of vinyl ethers.[10] Changes in Brønsted slopes represent second derivatives of log k with respect to basicity and can be described by the direct interaction coefficient p_y (eq 1) for curvature in a Brønsted slope, or by the cross-interaction coefficient p_{xy} (eq 2), for changes in Brønsted slopes

$$p_y = \partial\beta/-\partial pK_a^{BH} \quad (1)$$

$$p_{xy} = \partial\beta/\partial pK_a^{CH} = \partial\alpha/-\partial pK_a^{BH} \quad (2)$$

when the structures of both the carbon acid and the base catalyst are changed.[3] The available data for proton transfer to and from carbon indicate that the interaction coefficients are generally small, which corresponds to large curvatures of the energy surface at the saddle point for the reaction.[4]

The existence of changes in transition-state structure for proton abstraction from carbon has been questioned, however.[11-16] Several workers, notably Kemp[11] and Bordwell,[12,13] have commented on the lack of evidence for curvature in many Brønsted plots. Even when curvature is observed, it may be caused by changes in the rate-limiting step,[14,16,17] in solvation,[18,19] or in the

(1) This research was supported in part by grants from the National Institutes of Health (GM 20888) and the National Science Foundation (PCM 81-17816).

(2) Bell, R. P. *The Proton in Chemistry*, 2nd ed.; Cornell University Press: Ithaca, NY, 1973. Bell, R. P. *Symp. Faraday Chem. Soc.* **1975**, *10*, 7–19.

(3) (a) Jencks, D. A.; Jencks, W. P. *J. Am. Chem. Soc.* **1977**, *99*, 7948–7960. (b) Jencks, W. P. *Chem. Rev.* **1985**, *85*, 511–527.

(4) Thornton, E. R. *J. Am. Chem. Soc.* **1967**, *89*, 2915–2927. Harris, J. C.; Kurz, J. L. *J. Am. Chem. Soc.* **1970**, *92*, 349–355.

(5) Argile, A.; Carey, A. R. E.; Fukata, G.; Harcourt, M.; More O'Ferrall, R. A.; Murphy, M. G. *Isr. J. Chem.* **1985**, *26*, 303–312.

(6) Ahrens, M.-L.; Eigen, M.; Kruse, W.; Maass, G. *Ber. Bunsenges. Phys. Chem.* **1970**, *74*, 380–385.

(7) Kreevoy, M. M.; Oh, S.-W. *J. Am. Chem. Soc.* **1973**, *95*, 4805–4810.

(8) (a) Bell, R. P. *Proc. R. Soc. London, A* **1936**, *154*, 414. (b) Bell, R. P.; Lidwell, O. M. *Proc. R. Soc. London, A.* **1940**, *176*, 88–113.

(9) Bernasconi, C. F.; Hibdon, S. A. *J. Am. Chem. Soc.* **1983**, *105*, 4343–4348.

(10) Kresge, A. J.; Chen, H. L.; Chiang, Y.; Murrill, E.; Payne, M. A.; Sagatys, D. S. *J. Am. Chem. Soc.* **1971**, *93*, 413–423.

(11) Kemp, D. S.; Casey, M. L. *J. Am. Chem. Soc.* **1973**, *95*, 6670–6680.

(12) (a) Bordwell, F. G.; Boyle, W. J., Jr. *J. Am. Chem. Soc.* **1972**, *94*, 3907–3911. (b) Bordwell, F. G.; Boyle, W. J. *J. Am. Chem. Soc.* **1975**, *97*, 3447–3452.

(13) (a) Bordwell, F. G.; Hughes, D. L. *J. Org. Chem.* **1980**, *45*, 3314–3320. (b) Bordwell, F. G.; Hughes, D. L. *J. Am. Chem. Soc.* **1985**, *107*, 4737–4474. (c) Bordwell, F. G.; Branca, J. C.; Cripe, T. A. *Isr. J. Chem.* **1985**, *26*, 357–366.

(14) Johnson, C. D. *Chem. Rev.* **1975**, *75*, 755–765.

(15) Streitwieser, A. Jr.; Kaufman, M. J.; Bors, D. A.; Murdoch, J. R.; MacArthur, C. A.; Murphy, J. T.; Shen, C. C. *J. Am. Chem. Soc.* **1985**, *107*, 6983–6986.

(16) Eigen, M. *Angew. Chem., Int. Ed. Engl.* **1964**, *3*, 1–19.

(17) (a) Murdoch, J. R. *J. Am. Chem. Soc.* **1972**, *94*, 4410–4418. (b) Murdoch, J. R. *J. Am. Chem. Soc.* **1980**, *102*, 71–78.

(18) (a) Hupe, D. J.; Wu, D. *J. Am. Chem. Soc.* **1977**, *99*, 7653–7659. (b) Keefe, J. R.; Morey, J.; Palmer, C. A.; Lee, J. C. *J. Am. Chem. Soc.* **1979**, *101*, 1295–1297. (c) Jencks, W. P.; Brant, S. R.; Gandler, J. R.; Fendrich, G.; Nakamura, C. *J. Am. Chem. Soc.* **1982**, *104*, 7045–7051. (d) Jencks, W. P. *Adv. Chem. Ser.* **1987**, *215*, 155–167.

(19) Bernasconi, C. F.; Bunnell, R. D. *Isr. J. Chem.* **1985**, *26*, 420–427.

0002-7863/90/1512-1880$02.50/0